Development of an Adaptive Aero-Propulsive Performance Model in Cruise Flight – Application to the Cessna Citation X

Anca STEPAN[1], Georges GHAZI[1], Ruxandra Mihaela BOTEZ*,[1]

*Corresponding author
[1]LARCASE, Department of Automated Production Engineering,
École de technologie supérieure (ÉTS), University of Quebec,
1100 Notre Dame West, Montreal, Quebec, Canada, H3C 1K3,
anca.stepan.1@ens.etsmtl.ca, georges.ghazi@etsmtl.ca, ruxandra.botez@etsmtl.ca*

Abstract: *To accurately predict the amount of fuel needed by an aircraft for a given flight, a performance model must account for engine and airframe degradation. This paper presents a methodology to identify an aero-propulsive model to predict the fuel flow of an aircraft in cruise, while considering initial modeling uncertainties and performance variation over time due to degradation. Starting from performance data obtained from a Research Aircraft Flight Simulator, an initial aero-propulsive model was identified using different estimation methods. The estimation methods studied in this paper were polynomial interpolation, thin-plate splines, and neural networks. The aero-propulsive model was then structured using two lookup tables: one lookup table reflecting the aerodynamic performance, and another table reflecting the propulsive performance. Subsequently, an adaptive technique was developed to locally and then globally, adapt the lookup tables defining the aero-propulsive model using flight data. The methodology was applied to the Cessna Citation X business jet aircraft, for which a highly qualified level D research aircraft flight simulator was available. The results demonstrated that by using the proposed aero-propulsive performance model, it was possible to predict the aerodynamic performance with an average relative error of 0.99%, and the propulsive performance with an average relative error of 3.38%. These results were obtained using the neural network estimation method.*

Key Words: *Aero-Propulsive Performance, Neural Network, Adaptive Lookup Tables, Fuel Economy*

1. INTRODUCTION

The aviation industry is again experiencing a surge in air traffic following the COVID-19 pandemic crisis during the last two years. In a report published by the ICAO in October 2021, it was shown that the capacity in the number of seats worldwide was 40% lower in 2021 compared to 2019, and 50% lower in 2020 compared to 2019 [1]. This data reopens the discussion on a subject that is of concern to the population during several years: the climate impact of the aviation industry. An ICAO report shows that a significant development in air traffic is expected over the next few decades. Indeed, the increase in world trade, the importance of the tourism sector and the increase in population lead researchers to believe that there will be 3.3 times more flights in 2045 compared to 2015 [2]. Since the publication of the

report of the Intergovernmental Panel on Climate Change (IPCC) in 1999, the harmful effects of various chemicals have been identified: CO_2 input into the atmosphere causing global warming, while NO_x and SO_x emissions weakening the ozone. The ATAG estimated that in 2019, 915 million tons of CO_2 were released into the atmosphere due to aviation, which represented 2% of the total production of this greenhouse gas worldwide [3]. This is more than the worst-case scenario predicted in the IPCC report in 1999, which predicted 500 to 600 million tons per year during the same period [4]. Several strategies are currently being explored to address this problem, such as the use of sustainable fuels, the development of hydrogen engines, and the improvement of existing fuel-saving technologies.

Aircraft trajectory optimization is another promising solution for reducing aircraft fuel consumption and its associated emissions. Indeed, studies conducted by Dancila and Botez [5-7] and by Murrieta *et al.* [8], have shown that significant fuel savings can be achieved by optimizing the flight trajectory of an aircraft during the cruise phase. Since emissions are related to the amount of fuel burned by aircraft engines [9], a reduction in fuel consumption necessarily leads to a reduction in emissions. Nevertheless, it is important to specify that the quality of the results of the optimization process depends mainly on the quality of the mathematical model used to predict the trajectory of the aircraft. It is therefore crucial to have a reliable mathematical model that reflects the performance of the aircraft with a high degree of accuracy, otherwise the optimization results could be compromised.

Many studies have been conducted at the LARCASE laboratory to model the propulsive performance of an aircraft. For example, Rodriguez and Botez [10] and Ghazi and Botez [11] presented different techniques for developing a model to predict engine thrust and fuel flow. Dancila and Botez [12] proposed a new algorithm to predict engine thrust and fuel burn by considering the aircraft's center of gravity position in cruise. Hamel *et al.* [13] developed a method for identifying the flight dynamics of an aircraft using identification techniques, while Ghazi *et al.* [14] proposed a new methodology for identifying an aircraft performance model for Flight Management System (FMS) applications.

Although the results obtained in these studies were very good, none of them considered the aging (degradation) of the aircraft components over time. Indeed, it was estimated that an aircraft can increase its fuel consumption by approximately 2% every 5 years [15]. This statistic becomes less and less certain over time, which means that aircraft crews tend to overestimate the amount of fuel required for each flight, following the lack of an accurate picture of the current performance of the aircraft. This overvaluation causes significant economic losses for airlines, which assign about a quarter of their annual budget for fuel expenses. This overvaluation also has environmental issues since an increased use of fuel is synonymous with an increase in greenhouse gases in the atmosphere.

In this paper, we propose a new model representing the aerodynamic and propulsive performance of an aircraft. The study is a continuation of a previous work conducted by Ghazi *et al.* [16], in which only the aerodynamic model was adapted to account for initial modeling uncertainties and aircraft degradation. In this study, we propose to extend the work of Ghazi *et al.* [16] by considering the possibility of adapting the aerodynamic and propulsive model. This aspect allows to better monitor the global performance of the aircraft, thus enabling to detect whether the degradation comes from the airframe (i.e., aerodynamic) or the engine (i.e., propulsive). This new methodology was applied to the well-known Cessna Citation X business jet, for which a Research Aircraft Flight Simulator (RAFS) was available. The RAFS was designed and manufactured by CAE Inc. and has the lightest level-D qualification for its flight dynamics and propulsion models. Figure 1 shows a picture of the RAFS, while Table 1 lists several specifications of the Cessna Citation X.

Figure 1: Cessna Citation X Research Aircraft Flight
Simulator (RAFS)

Table 1: Main dimensions and specifications of
the Cessna Citation X

Aircraft caracteristics	Value
Height	5.85 m
Width	21.1 m
Length	22.43 m
Wing area	48.9 m^2
Wing sweep	37 degrees
Maximum weight at take-off	16602 kg
Maximum altitude	15545 m
Maximum Speed	Mach 0.935
Engine type (2)	Rolls-Royce AE3007C2
Maximum takeoff thrust	30.09 kN

The remainder of this paper is as follows: Section 2 explains the development of the initial aerodynamic and propulsive performance models, Section 3 details how the algorithm uses flight data to locally adapt the performance models, Section 4 gives with the global adaptation of the performance models. Finally, the paper ends with a conclusion and remarks.

2. INITIAL PERFORMANCE MODEL

The first step in the methodology was to create an initial performance model for predicting the aero-propulsive parameters of the Cessna Citation X.

The strategy consisted in designing the performance model, and in dividing it into two separate and independent sub-models, including: one sub-model reflecting the aerodynamic performance of the aircraft, and another sub-model reflecting the propulsive characteristics. In addition, it was decided to create the two sub-models using adaptive lookup tables. Indeed, as the linearity of the aerodynamic and propulsive performances is not guaranteed, lookup tables are a good approach to represent the data without having a mathematical equation. Another advantage of lookup tables is the computational time required to obtain an output. Their disadvantage, on the other hand, is the storage space and memory that they might require.

However, in this paper, both performance models consider only two input variables. Therefore, the two lookup tables have relatively simple two-dimensional structures, and do not require much memory for data storage. The aerodynamic model is based on the simplified free-body diagram of an aircraft in cruise as shown on Fig. 2.
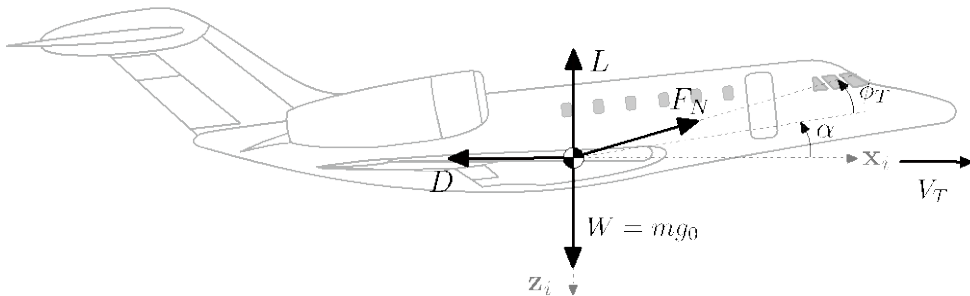

Figure 2: Forces acting on an aircraft in cruise phase

By assuming that in cruise the angle of attack (α), as well as the engine inclination angle (ϕ_T), are very small, it can be considered that the drag (D) is equal to the thrust (F_N). This simplification allows to postulate the main relationship that drives the aerodynamic performance model, namely:

$$D = F_N \tag{1}$$

Another important relationship is the one between the drag and the lift. Figure 3 shows the typical variation of the drag coefficient as a function of the lift coefficient and Mach number [17]. Mathematically, the following relationship can be therefore written:

$$CD_s = f_1(CL_s, M) \tag{2}$$

where CD_s is the drag coefficient, CL_s is the lift coefficient, M is the Mach number, and f is an unknown function to be determined from available flight data.

The third relationship to consider is the one between the thrust and the fan speed (N_1). For this purpose, Figure 4 shows the typical variation of the corrected thrust as function of the corrected fan speed and Mach number [17]. Based on the data shown in this figure, and the work done by Ghazi and Botez in [18], the following mathematical relationship can be defined:

$$\frac{F_N}{\delta} = f_2\left(\frac{N_1}{\sqrt{\theta}}, M\right) \tag{3}$$

where N_1 is the engine fan speed, δ and θ are the pressure and temperature ratios, respectively.

By combining the three relationships in Eqs. (1) to (3), the following relationships can be obtained:

$$\frac{N_1}{\sqrt{\theta}} = f_3(CL_s, M) \tag{4}$$

where the lift coefficient CL_s can be estimated as follows:

$$CL_s = \frac{W}{0.5\rho S V_T^2} \tag{5}$$

where W is the aircraft weight, ρ is the air density, S is the aircraft wing area, and V_T is the aircraft true airspeed.
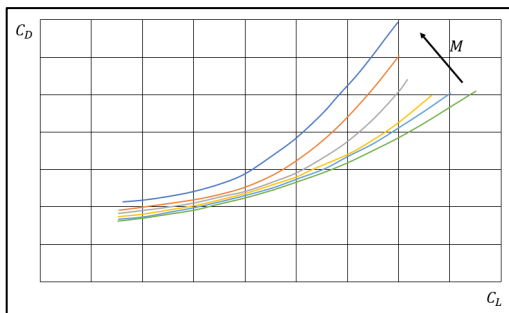

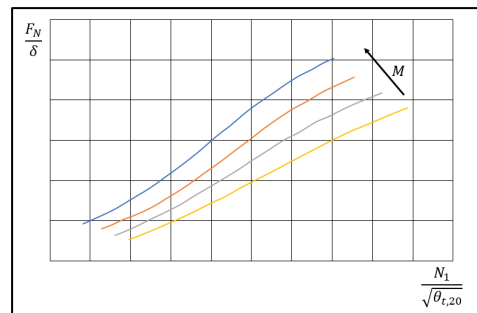Figure 3: Illustration of the dependency between the drag coefficient and the lift coefficient

Figure 4: Illustration of the dependency between the thrust and the fan speed of an engine

It should be noted that Eq. (4) involves the fan speed N_1, which is actually an engine parameter. However, since the main assumption is that the drag is equal to the thrust, it can be therefore considered that the fan speed N_1 can be a good estimator of the amount of drag

needed to balance the aircraft in cruise. To complete the aero-propulsive model, it is necessary to add another relationship to describe the performance of the engine. In general, for the cruise phase, the engine performance of interest is primarily the fuel flow. According to ESDU [19] and to Ghazi and Botez [18], the fuel flow of a turbofan engine can be approximated in corrected form using the following relationship:

$$\frac{W_F}{\delta\sqrt{\theta}} = f_4\left(\frac{N_1}{\sqrt{\theta}}, M\right)$$
(6)

where W_F is the engine fuel flow, and $W_F/\delta\sqrt{\theta}$ is the corrected engine fuel flow.

Finally, the aero-propulsive performance model explained in the rest of this paper can be summarized by the two following equations:

$$\frac{N_1}{\sqrt{\theta}} = f(CL_S, M) \qquad \leftarrow \text{Aerodynamic Performance}$$
(7a)

$$\frac{W_F}{\delta\sqrt{\theta}} = f\left(\frac{N_1}{\sqrt{\theta}}, M\right) \qquad \leftarrow \text{Propulsive Performance}$$
(7b)

Once the core equations describing the aircraft aero-propulsive model were defined, the next step was to identify the mathematical functions defining the model, and then to restructure these functions into a lookup table.

The data chosen to identify the functions in Eqs. (7a) and (7b) and then create the aero-propulsive lookup tables was obtained from the Cessna Citation X Flight Crew Operating Manual (FCOM). The FCOM is one of the aircraft flight manuals, and contains data describing the fuel flow required to operate the aircraft in cruise for a wide range of flight conditions, and by assuming zero degradation. Thus, using the data published in FCOM, and combining them with the equations (7a) and (7b), the two data sets shown in Fig. 5 were obtained. Figure 5(a) shows the variation of the corrected fan speed as a function of the lift coefficient and the Mach number, while Fig. 5(b) shows the variation of the corrected fuel flow as a function of the corrected fan speed and the Mach number.
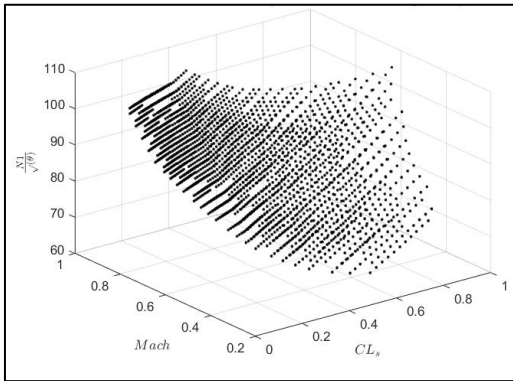
a) Corrected fan speed as function of lift coefficient and Mach number
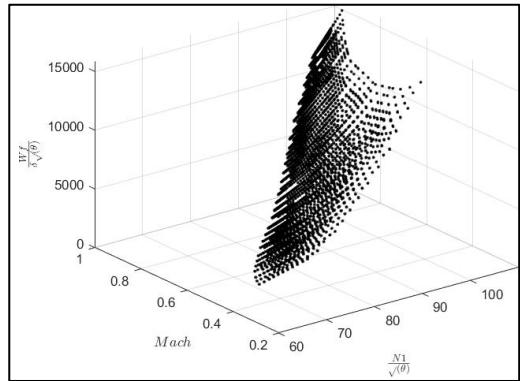
b) Corrected engine fuel flow as function of corrected fan speed and Mach number

Figure 5: FCOM flight data for aerodynamic and propulsive models

Three methods were tested and compared to interpolate the data presented in Fig. 5(a) and 5(b), and thus obtain the initial performance model. These methods were: (1) polynomial interpolation, (2) thin-plate spline, and (3) neural networks.

Based on a statistical comparison, the polynomial equation used to create the two lookup tables was of order 2 for each input variable.

It should be noted that attempts to fit the FCOM data with high polynomial orders led to better results, but the obtained surfaces were irregular (i.e., not smooth), which was a sign of overfitting.

For the neural network interpolation, the following parameters were used to train the network:

- A total of 926 sets of data were used to train both neural networks (one for the aerodynamic model, and one for the propulsive model). In addition, 70% of this is considered for the training, and 30% for the test.
- The activation function used for both neural networks was the sigmoid function.
- Each neural network consisted of a single hidden layer. This choice was made based on the principle that a neural network with a single hidden layer was enough to model all continuous functions on a specific domain, as long as this hidden layer had enough nodes (i.e., neurons) [20].
- The optimal number of nodes on the hidden layer was found by increasing the number of nodes from 1 to 15, and by computing the resulting relative error, as shown in Figure 6. As can be seen on this figure, the bests results were obtained for 4 nodes for the aerodynamic model, and for 8 nodes for the propulsive model.
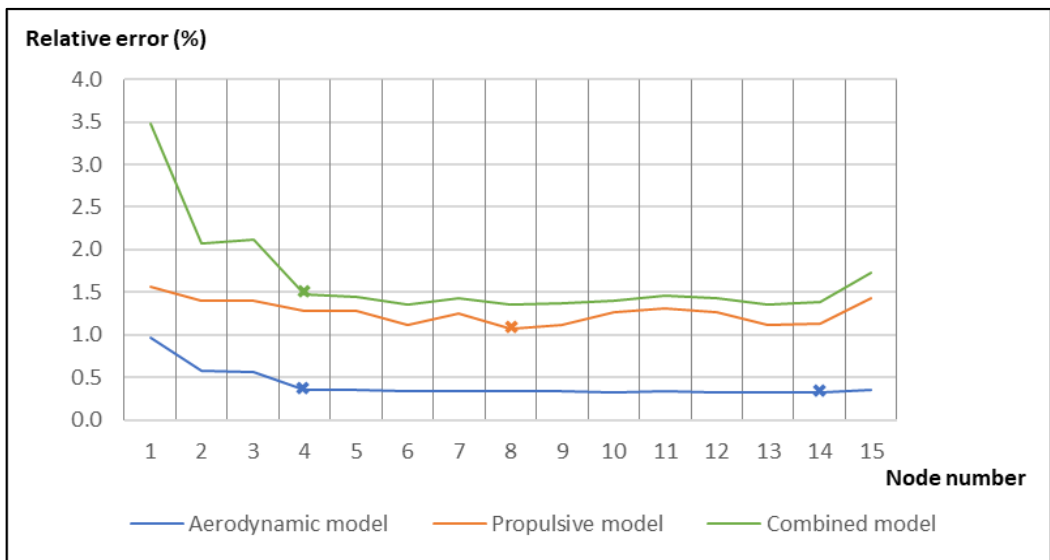

Figure 6: Evolution of average relative error for the initial performance models
depending on the number of nodes in the hidden layer

Table 2 presents the mean relative error obtained by comparing the reference data published in the FCOM with that calculated from the lookup tables created for the initial aero-propulsive model using the three interpolation methods.

It should be noted that in the combined model is not an aerodynamic and propulsive model combination.

The $N_1/\sqrt{\theta}$ value for the propulsive model is coming from the aerodynamic lookup table, instead of coming from the data published in the FCOM.

Table 2: Comparison between average relative error obtained through three
estimation methods to create the initial lookup tables

Method	Performance Model	Mean Relative Error
Polynomial interpolation	Aerodynamic	0.99%
	Propulsive	2.01%
	Combined	4.30%
Thin-plate spline	Aerodynamic	0.34%
	Propulsive	1.26%
	Combined	1.40%
Neural Network	Aerodynamic	0.36%
	Propulsive	1.30%
	Combined	1.50%

From these results, we can conclude that the combined performance model is highly impacted by the aerodynamic and the propulsive model. Since the combined model, which is a propulsive performance lookup table, uses data provided by the aerodynamic lookup table and by the propulsive model (except for $N_1/\sqrt{\theta}$), it is normal that its mean relative error will be much higher than that of the two models on which it is based on. Also, the neural network and the thin-plate spline are the estimation methods that gave the closest results to the FCOM data. With a very low mean relative error for the aerodynamic model and propulsive one, the resulted combined model mean relative error can be as low as 1.40% and 1.50%, compared to the 4.3% generated with the polynomial interpolation.

Finally, two additional lookup tables were created to keep track of each node, and of the number of times a node was modified. These lookup tables reflect a confidence coefficient λ, which is set as an initial value of 1 ($\lambda_{x,y} = 1, \forall\{x, y\}$). The value of the confidence coefficient is updated with every iteration of an adaptation of a node.

3. LOCAL ADAPTATION OF LOOKUP TABLES

Once the initial lookup tables were created, the next step was to develop an algorithm to adapt them "locally" by using flight test data.

The data used to develop this algorithm was generated from the RAFS available at the LARCASE laboratory. For this purpose, several cruise tests were performed with the RAFS, and a total of 10,113 data sets were collected for a wide range of operating conditions to cover as much as possible the aircraft's flight envelope. The data was then filtered and averaged to obtain the cruise performance of the aircraft, using the method described by Ghazi, et al. [16]. Finally, the lookup tables can be locally adapted, as illustrated in Figure 7, and using the procedure described in the following paragraph.

Before starting the adaptation process, it is necessary to determine which lookup table needs to be adapted. Indeed, always adapting the aerodynamic and propulsive lookup table is not necessarily the best strategy to maintain the accuracy of the entire model. In this paper, a logic based on 6 situations is proposed to determine the accuracy of each lookup table, and then to identify which one should be adapted:

- **Situation 1:** Adapting only the aerodynamic performance model;
- **Situation 2:** Adapting only the propulsive performance model;
- **Situation 3:** Adapting both performance models at any time;

- **Situation 4:** Adapting the model with the largest relative error;
- **Situation 5:** Adapting the lookup tables only when a relative error is higher than 1% (for aerodynamic model) and 2% (for propulsive model) is detected. These limits were set based on the initial performance models mean relative errors compared to the FCOM data;
- **Situation 6:** Adapting the lookup tables based on the Specific Range Method (SRM). This method is based on a study made by Airbus, describing a performance monitoring technique using the Specific Range parameters [21]:

$$SR = \frac{a_0 \left(M \frac{L}{D} \right)}{\left(\frac{SFC}{\sqrt{\theta}} \right) mg} = \frac{V_T \left(\frac{L}{D} \right)}{\left(\frac{SFC}{\sqrt{\theta}} \right) mg} = \frac{V_T}{W_f} \tag{8}$$

where SR is the specific range, a_0 is the speed of sound at sea level, SFC is the specific fuel consumption, and m is the aircraft's mass.

This equation is interesting because it combines both aerodynamic (ML/D) and propulsive $\left(SFC/\sqrt{\theta} \right)$ parameters. The SR can also be written as follows: $(SR = V_T/W_F)$. As the True Airspeed (V_T) remains constant in cruise, it is possible to correlate the aircraft performance (SR) with the fuel flow (W_f).
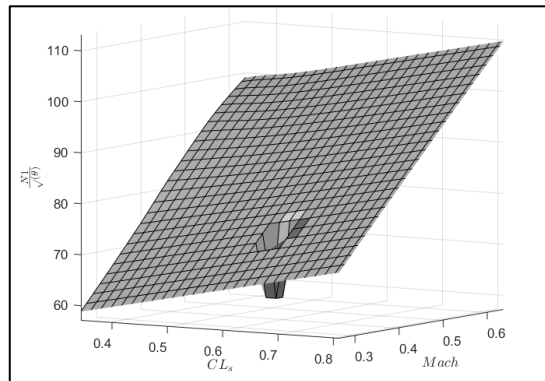

Figure 7: Example of local adaptation for the aerodynamic lookup table

In addition, the aircraft fuel flow for a given flight condition can be determined in three ways:

- Through flight test data (i.e., measured);
- Through the propulsive lookup table by using interpolation with the measured N_1 (i.e., calculated);
- By using the interpolated N_1 from the aerodynamic performance model as an input to the propulsive lookup table (i.e., theorical).

By comparing the three different fuel flow values (i.e., measured, calculated, and theorical), it is possible to conclude where the deterioration is coming from, based on the following procedure:

1. Discrepancy between the *measured* and *calculated* fuel flows means a deterioration of the engines (i.e., propulsive model) & propulsive model should be adapted;
2. Discrepancy between the *calculated* and *theorical* fuels flows means a deterioration of the airframe (i.e., aerodynamic model) and aerodynamic model should be adapted;
3. Discrepancy between the *theorical* and *measured* fuels flows means a possible global deterioration of the aircraft, and both performance models should be adapted.

These situations determine which performance model will be locally adapted for every iteration of the following algorithm. The mathematical algorithm developed to locally adapt the lookup table is shown in Algorithm 1.

Algorithm 1: Local adaptation method

1. Extract a flight point $\{x, y, z\}$ from the RAFS (where $\{x, y, z\} = \{N_1/\sqrt{\theta}, M, CL_s\}$ for the aerodynamic model, and $\{x, y, z\} = \{N_1/\sqrt{\theta}, M, W_F/\delta\sqrt{\theta}\}$ for the propulsive model design.

2. Perform a bilinear interpolation to find the lookup table value for the function f at the point $\{x, y\}$. The bilinear interpolation is defined as follows:

$$f(x,y) = \frac{1}{(x_2 - x_1)(y_2 - y_1)} [x_2 - x \quad x - x_1] \begin{bmatrix} f(x_1, y_1) & f(x_1, y_2) \\ f(x_2, y_1) & f(x_2, y_2) \end{bmatrix} \tag{9}$$

where the x_1 and x_2 are the breakpoints on the x −axis that surround the input flight data, y_1 and y_2 values are the breakpoints on the y-axis that surround the input flight test data, and $f(x_{\{1,2\}}, y_{\{1,2\}})$ are the values of the lookup table for the four nodes surrounding the input flight test data.

3. Compute the Euclidian distance between the flight test data and the node breakpoints with the following formula:

$$d_{[i,j]} = \sqrt{(x - x_i)^2 + (y - y_j)^2} \tag{10}$$

where $i = \{1,2\}$ and $j = \{1,2\}$.

4. Normalize the Euclidian distance by dividing the diagonal of the quadrilateral created by the 4 nodes (x_i, y_j) around the flight test data (x, y), as follows:

$$\delta_{[i,j]} = \frac{d_{[i,j]}}{\sqrt{(x_2 - x_1)^2 + (y_2 - y_1)^2}} \tag{11}$$

5. Compute the new node value z^+ based on the flight test data z, and the on current node value z^-, using the following rule:

$$z^+ = k_c z^- + k_a z \tag{12}$$

where k_c and k_a are the conservative and adaptive gain, respectively. These two gains are calculated using the following relationships:

$$k_c = \left(\frac{\delta_{i,j} - \delta_{i,j}^{\lambda_{i,j}}}{1 - \delta_{i,j}^{\lambda_{i,j}}} \right) \quad \text{and} \quad k_a = \left(\frac{1 - \delta_{i,j}}{1 - \delta_{i,j}^{\lambda_{i,j}}} \right) \tag{13}$$

These gains represent the proportion of the old value that is kept (conservative) and the proportion of the new value that is considered (adaptative gain). The sum of k_c and k_a is always equal to 1.

6. Finally, the confidence coefficient is updated with this equation: $\lambda_{i,j}^+ = \lambda_{i,j}^- + (1 - \delta_{i,j})$.

With the procedure describe in Algorithm 1, the closer a flight test data is to a node coordinates, the greater the adaptative gain and the closer the new node value will be to the flight test data. This algorithm is repeated each time a new data set is obtained from the RAFS.

4. GLOBAL ADAPTATION OF LOOKUP TABLES

In the previous section, a method for locally fitting the lookup tables defining the aero-propulsive model was presented. This method fits the models by locally deforming the surface corresponding to each lookup table. Although very effective, this method unfortunately introduces irregularities that result in a non-smooth surface (as shown in Figure 7). Thus, to correct the result, a global adaptation is necessary.

Basically, the global adaptation method uses nodes that have already been locally adapted to adjust the general trend of the rest of the lookup table. The number of locally adapted nodes relative to the total number of nodes must be greater than 10% for the global adaptation process to be completed. Below this threshold, there is not enough collected data to generalize the adaptation to the entire lookup table data. In the same way as for the design of the initial model, in

Figure 8: Neural network architectures for the global adaptation of the aerodynamic and propulsive lookup tables

Section 2, three estimation methods were used to perform the global adaptation: (1) polynomial interpolation, (2) thin-plate spline, and (3) neural networks. For the polynomial interpolation, weights can be attributed to every node that has been locally adapted. These weights are the values of the confidence coefficients (λ) associated to each node. When $\lambda = 1$, for which a node has not been adapted, this node has less impact in the overall adaptation process than a node that has already been adapted ($\lambda > 1$). In the neural network method, the weights are introduced as input values to the training process, along with the input values, as shown in Figure 8. The neural network parameters are the same as those used to develop the initial performance model in Section 2. The lookup tables produced by all three estimation methods have close values. Figure 9 illustrates an example of lookup tables obtained by the neural network estimation method. Figure 9(a) shows the aerodynamic model, and Figure 9(b) presents the propulsive model.
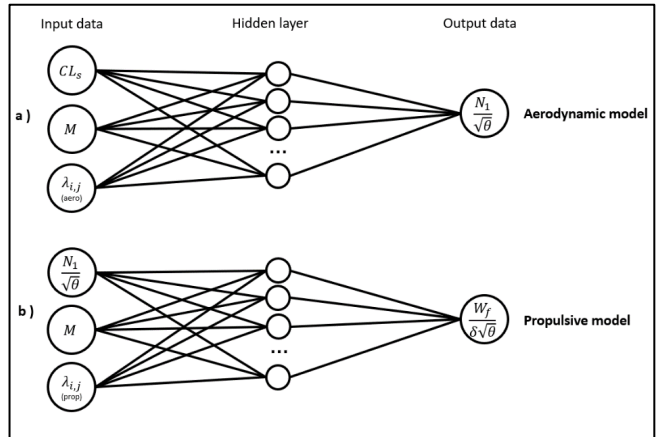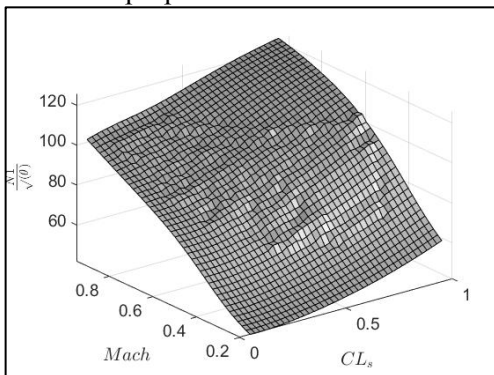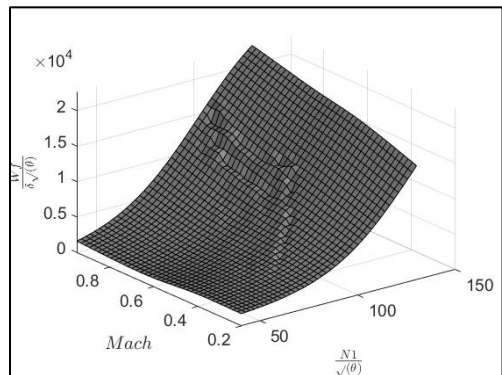

a) Aerodynamic model b) Propulsive model

Figure 9 : Adapted lookup tables through the neural network estimation method

Table 3 gives the mean relative error for each adaptation situation considered in the polynomial interpolation method. For the other estimation methods, the results are considered fairly similar. In addition, the polynomial interpolation method has the lowest computing time among all three methods.

Table 3: Mean relative error for the aero-propulsive performance models after
doing a global adaptation using polynomial interpolation

Situation	Mean Relative Error [%]			Computing Time [s]
	Aerodynamic Model	Propulsive Model	Aero-Propulsive Combined Model	
Initial model	12.11	10.00	32.18	N/A
Situation 1	1.13	10.00	12.35	101.27
Situation 2	12.11	4.74	33.37	123.01
Situation 3	**0.99**	4.11	6.66	52.44
Situation 4	**0.99**	4.02	**5.32**	77.84
Situation 5	**0.99**	3.99	6.56	48.31
Situation 6	**0.99**	4.11	6.65	50.84

As shown in Table 3, the adaptation situations giving the best results are the situations 4 and 5, i.e., the adaptation of the lookup table with the largest mean relative error and the adaptation of the lookup tables with a relative error greater than 1% (for the aerodynamic model) or 2% (for the propulsive model).

5. VALIDATION AND RESULTS

This section presents several analyses and comparisons for the validation of the proposed methodology to adapt locally and globally the two lookup tables defining the aero-propulsive model.

5.1 Validation of the Methodology

The validation of the methodology was done using datasets obtained from the Cessna Citation X RAFS in cruise flight. The conditions are the same as the ones for the datasets used in the adaptation algorithm. The input data used for the validation is shown in Fig. 10. Thus, each input data collected from the RAFS was fed into Algorithm 1 to adapt the two lookup tables defining the performance model. This adaptation process led to the two new lookup tables shown in Fig. 9.
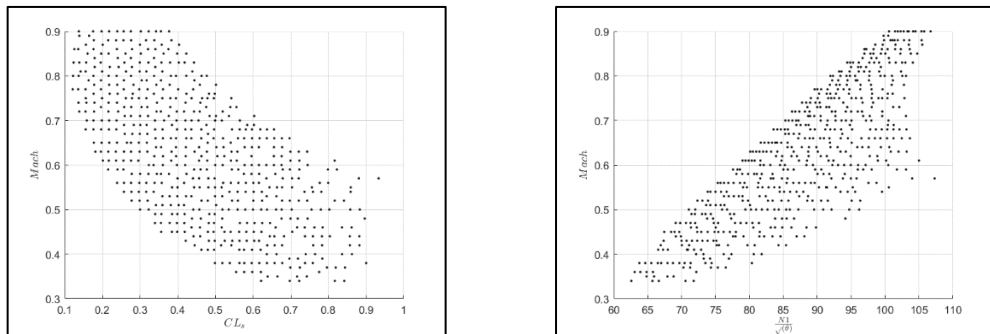

Figure 10: Input data for aerodynamic and propulsive models used for validation of algorithm

The criteria used to compare the estimation methods for all 3 situations, as well as to validate the whole adaptation algorithm was the mean relative error.

Figure 11 presents this information for every performance model for situation 3 to 6. Using the neural network method, the best results were expressed in terms of the mean relative error which in the situation 5 is the lowest. In addition, the obtained surfaces are smoother using this method than thin-plate splines and polynomial interpolation.

	Initial	FCOM	Situation 3		Situation 4		Situation 5		Situation 6	
	%	%	%		%		%		%	
				% improv.		% improv.		% improv.		% improv.
Average relative error (aerodynamic model)	11.11	0.36	1.01	90.94	1.07	90.36	0.99	91.05	1.01	90.94
Average relative error (propulsive model)	11.26	1.30	3.75	66.68	4.01	64.39	3.38	69.95	3.75	66.68
Average relative error (combined model)	36.61	1.50	6.25	82.92	6.05	83.48	6.25	82.93	6.25	82.92

Figure 11: Mean relative error using neural networks for situations 3 through 6 and their percentage of improvement compared to the initial performance models

5.2 Influence of the Initial Model Uncertainties

The second analysis consisted in verifying the efficiency of the adaptation algorithm according to the accuracy of the initial model. The objective was to validate that the adaptation algorithm can produce results close to the actual aircraft performance regardless of the initial discrepancy between the initial lookup tables and the flight test data. For this purpose, constant values were added to the initial lookup tables to bias them. Thus, different bias values ranging from 0 to 10% RPM in 2% RPM steps were simulated for the aerodynamic model, and between 0 lb/h and 1000 lb/h with a 200 lb/h steps for the propulsive model.
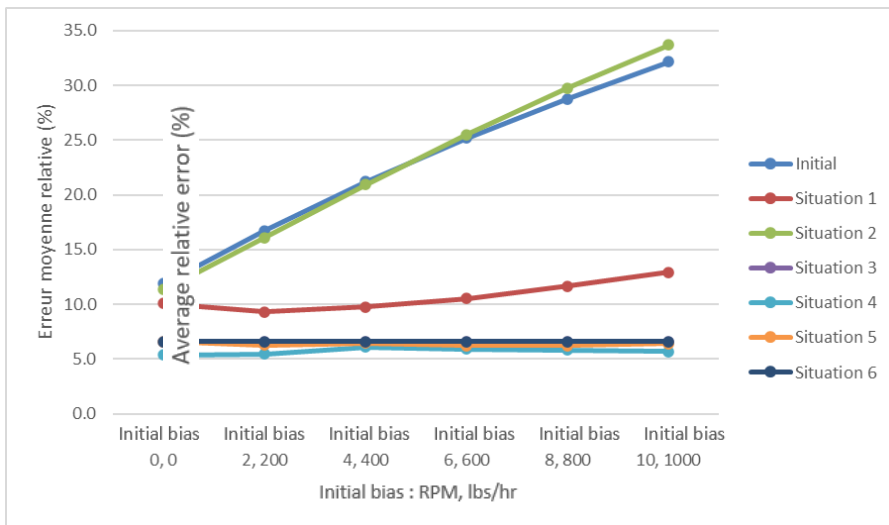

Figure 12: Mean relative error with different initial bias on initial performance models (using polynomial interpolation)

Figure 12 shows the impact of adding an initial bias on the mean relative error for the aero-propulsive combined model with the polynomial interpolation estimation method.

The mean error for the initial lookup table increases linearly with the value of the added bias. This was expected, as increasing the value of the bias means shifting the values of the

lookup table upward. A similar observation can be made for situations 1 and 2, which can be explained by the fact that for these two situations, one of the two lookup tables is never adapted. However, it is interesting to mention that the average error increases much more in situation 2 than in situation 1. This aspect highlights the fact that the model is more sensitive to uncertainties on its propulsive part than on its aerodynamic part.

For the other situations, the mean relative error remains constant regardless of the bias's values introduced on the initial model. This result proves that the adaptation algorithm was able to correct the uncertainties of the initial model despite biases up to 10%RPM and 1000 lb/hr. This result was expected, and it was the same obtained using all three estimation methods and for all models (i.e., aerodynamic, propulsive, and combined).

Influence of the Number of Nodes for Local Adaptation

The third analysis that may be interesting to perform concerns the size of the area (i.e., the number of nodes) that is modified during the local adaptation process. Indeed, as explained in Section 3, the local adaptation process typically consists in modifying the four nodes of a lookup table that surrounds a flight condition. As a result, the area of the lookup table that is modified is delimited by four nodes. It may therefore be interesting to examine how the number of nodes (i.e., the size of the area) may affect the adaptation process. Thus, for this analysis, results obtained for three number of nodes were compared: 4 nodes, 16 nodes and 36 nodes.

Figure 13 presents a comparison between the mean relative error for an area of adaptation of 4, 16 and 36 nodes. It should be noted that this comparison was done for all three estimation methods, however, for the sake of clarity, only the results for the thin plate are presented in this figure. The same results were obtained for the other two estimation methods.
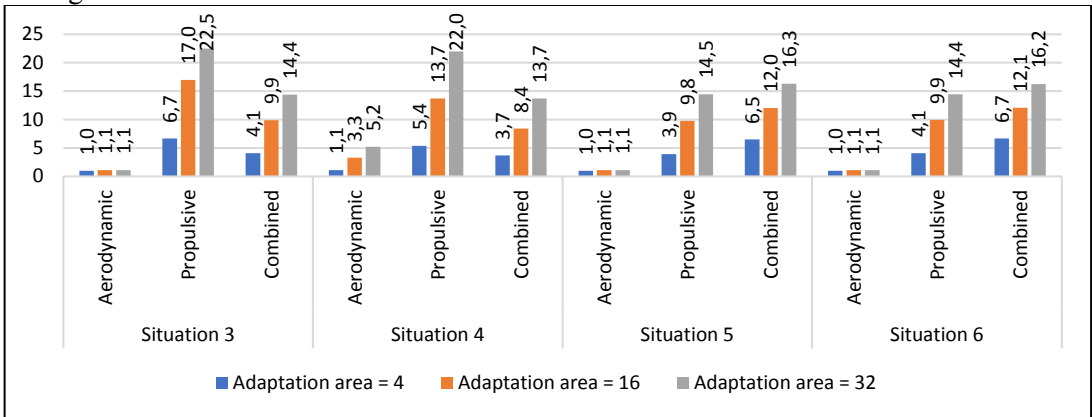

Figure 13: Average relative error depending on area of adaptation after global adaptation using polynomial interpolation

In Figure 13, the larger the adaptation area, the higher is the mean relative error. This result can be explained by the fact that increasing the area to be adapted allows more nodes to be impacted in the lookup table.

However, this adaptation adds a penalty, which results in less changes of the lookup table values at the adapted nodes.

Therefore, even if the table is modified, the modification is not sufficient to allow a more accurate result.

Based on this analysis, it can be concluded that the area of adaptation should correspond to 4 nodes.

5.3 Influence of the Number of Breakpoints

Finally, the last analysis consisted in evaluating the influence of the number of breakpoints. Indeed, the number of breakpoints is an important parameter because it defines the size of a lookup table grid. In general, it is important to have a grid that is fine enough to have a good fit that will correspond to the actual flight data, but also coarse enough to have a low computation time. For this purpose, the number of breakpoints was varied in this study from 30 to 80 for every adaptation situation and every estimation method. An example, of results for the propulsive model using thin-plate spline is given in Figure 14.
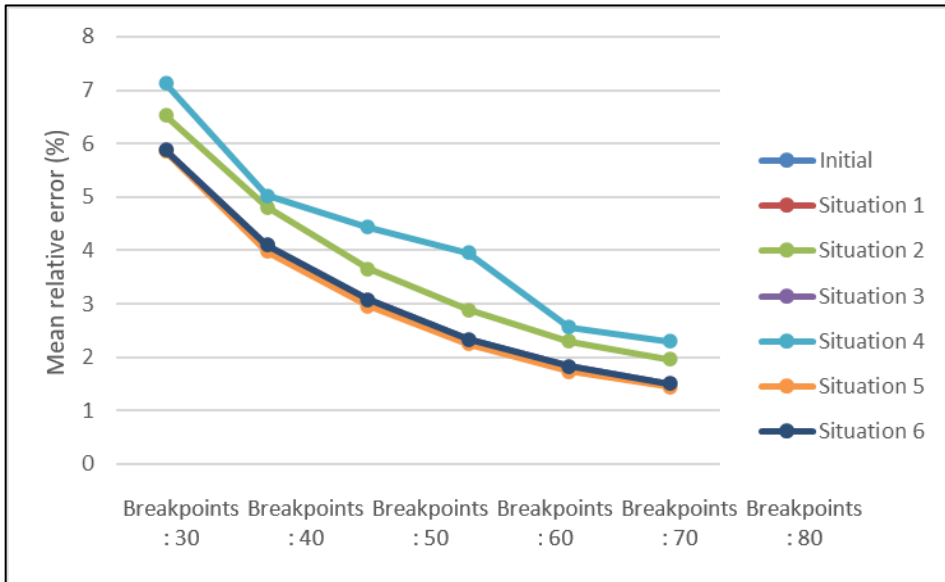

Figure 14: Mean relative error depending on number of breakpoints on an axis after a global adaptation using thin-plate spline

As expected, the more breakpoints there are, the finer is the grid and the relative error generally decreases more. At each step of 10, the average relative error decreases by about 1% on average. This aspect means that the size of the grid is an important factor influencing the algorithm results. Since the number of nodes increases with the number of breakpoints, but the number of flight data sets is the same, less information is used in the local adaptation process per node. Therefore, every set of flight data has a higher impact on an adaptation iteration. This impact is directly linked to the confidence coefficient, which increases with a local adaptation iteration, which allows the next iteration to have smaller impact on the result.

6. CONCLUSIONS

We present in this research an algorithm making the aerodynamic and propulsive performance prediction of a Cessna Citation X aircraft. Indeed, following this performance degradation over time, it becomes difficult to predict the quantity of fuel necessary in flight. This degradation model concluded through this research needs three stages to obtain its final performance prediction engine model.

This research presents a new approach to performance monitoring and prediction by targeting the causes of performance deterioration. Indeed, by use of two different models for the aerodynamic and propulsive performances, we are able not only to tell that the fuel

consumption is increasing, but also to point to the culprit, which is done through three different estimation methods: polynomial interpolation, thin-plate spline and neural networks. The best results were obtained using the neural network method, with a mean relative error of 0.99% for the aerodynamic model, 3.38% for the propulsive model and 6.25% for the combined model. The data used to obtain these results are provided by a Cessna Citation X flight simulator.

For future work, it would be interesting to explore methods for estimating lookup tables, more specifically during the ''global adaptation process''. Indeed, the first data having the most impact on the local adaptation of a node were also given as the inputs to the algorithm (refer to Section 2 for the mathematical algorithm). The data with the highest influence on the results should always be the last data to enter the algorithm since it is the most representative of the current performance of the aircraft.

REFERENCES

[1] T. Hasegawa, S. Chen and L. Duong, *Effects of Novel Coronavirus (COVID-19) on Civil Aviation : Economic Impact Analysis*, ICAO, Montréal, Canada, October 5th 2021.

[2] * * * ICAO, *ICAO Global Environmental Trends – Present And Future Aircraft And Emissions,* Working Paper, July 5th 2019.

[3] * * * ATAG, *Facts & Figures*, https://www.atag.org/component/factfigures/?Itemid.

[4] * * * IPCC, *Aviation and the Global Atmosphere*, 1999.

[5] R. M. Botez and B. Dancila, Vertical Flight Path Segments Sets for Aircraft Flight Plan Prediction and Optimization, *Aeronautical Journal*, vol. **122**(1255), pp. 1371-1, 2018.

[6] R. M. Botez and R. Dancila, Vertical Flight Profile Optimization for a Cruise Segment with RTA Contraints, *The Aeronautical Journal,* vol. **123**(1265), pp. 970-992, 2019.

[7] R. M. Botez and R. Dancila, New Flight Trajectory Optimization Method using Genetic Algorithms, *Aeronautical Journal,* 2021.

[8] H. Ruiz, A. Murrieta-Mendoza and R. Botez, Particle Swarm Optimization with Required Time of Arrival Constraint for Aircraft Trajectory, *SAE Aerospace,* vol. **13**(2), no. Innovation for Sustainable Aviation, pp. 269-291, 2020, doi: 10.4271/01-13-02-0020.

[9] G. Ghazi and R. M. Botez, Aircraft Mathematical Identification for Flight Trajectories and Performance Analysis in Cruise, *Journal of Aerospace Information Systems,* vol. **19**(8), pp. pp.1-20, 2022.

[10] L. Rodriguez-Fajardo and R. M. Botez, Generic new modeling technique for turbofan engines thrust, *The Journal of Aircraft Engineering ASCE,* vol. **29**(6), pp. 1492-1495, 2013.

[11] G. Ghazi and R. M. Botez, Identification and Validation of an Engine Performance Database Model for the Flight Management System, *AIAA Journal of Aerospace Information Systems,* no. **16**(8), pp. 1-45, 2019.

[12] B. Dancila, D. Labour and R. M. Botez, Fuel burn prediction algorithm for cruise, constant speed and level flight segments, *The Aeronautical Journal,* vol. **117**, no. 1191, pp. 491-503, 2013.

[13] A. Sassy, C. Hamel and R. M. Botez, Cessna Citation X aircraft global model identification from flight tests, *SAE International Journal of Aerospace,* vol. **6**(1), pp. 106-114, 2013, doi: 10.4271/2013-01-2094.

[14] S. Domanti, G. Ghazi and R. M. Botez, *New Methodology to Identify an Aircraft Performance Model for Flight Management System Applications*, AIAA Journal of Aerospace Information Systems, no. 17(6), pp. 249-310, 2020.

[15] * * * Airbus, *Getting Hands-on Experience with Aerodynamic Deterioration*, vol. 2, 2001.

[16] G. Ghazi, B. Gerardin, M. Gelhaye and R. M. Botez, *N*ew Adaptive Algorithm Development for Monitoring Aircraft Performance and Improving Flight Management System Predictions, *Journal of Aerospace Information Systems,* vol. **17**, pp. 1-16, 12/20 2019, doi: 10.2514/1.I010748.

[17] T. M. Young, *Performance of the Jet Transport Airplane: Amalysis Methos, Flight Operations and Regulations* (Aerospace Series), 2017.

[18] G. Ghazi and R. M. Botez, Identification and validation of an engine performance database model for the flight management system, *Journal of Aerospace Information Systems,* vol. **16**(8), pp. 307-326, 2019.

[19] * * * ESDU, *Non-dimentional approach to engine thrust and airframe drag for the analysis of measured performance data : aircraft with turbo-jet and turbo-fan engines*, ed. ESDU, 1970.

[20] A. Kratsios, *Universal Approximation Theorems*, Springer, 2019.

[21] * * * Airbus, *Getting to Grips with Aircraft Performance Monitoring*, Cedex, France, 2002.